Phosphorylation of OPTN by TBK1 enhances its binding to Ub chains and promotes selective autophagy of damaged mitochondria

Benjamin Richter[a], Danielle A. Sliter[b], Lina Herhaus[a], Alexandra Stolz[a], Chunxin Wang[b], Petra Beli[c], Gabriele Zaffagnini[d], Philipp Wild[a,1], Sascha Martens[d], Sebastian A. Wagner[e], Richard J. Youle[b], and Ivan Dikic[a,f,g,2]

[a]Institute of Biochemistry II, Goethe University School of Medicine, 60590 Frankfurt, Germany; [b]Biochemistry Section, Surgical Neurology Branch, National Institute of Neurological Disorders and Stroke, National Institutes of Health, Bethesda, MD 20892; [c]Institute of Molecular Biology, 55128 Mainz, Germany; [d]Max F. Perutz Laboratories, Vienna Biocenter, University of Vienna, 1030 Vienna, Austria; [e]Department of Medicine, Hematology/Oncology, Goethe University, 60590 Frankfurt, Germany; [f]Buchmann Institute for Molecular Life Sciences, Goethe University, 60438 Frankfurt, Germany; and [g]Institute of Immunology, School of Medicine, University of Split, 21 000 Split, Croatia

Edited by Brenda A. Schulman, St. Jude Children's Research Hospital, Memphis, TN, and approved February 23, 2016 (received for review December 4, 2015)

Selective autophagy of damaged mitochondria requires autophagy receptors optineurin (OPTN), NDP52 (CALCOCO2), TAX1BP1, and p62 (SQSTM1) linking ubiquitinated cargo to autophagic membranes. By using quantitative proteomics, we show that Tank-binding kinase 1 (TBK1) phosphorylates all four receptors on several autophagy-relevant sites, including the ubiquitin- and LC3-binding domains of OPTN and p62/SQSTM1 as well as the SKICH domains of NDP52 and TAX1BP1. Constitutive interaction of TBK1 with OPTN and the ability of OPTN to bind to ubiquitin chains are essential for TBK1 recruitment and kinase activation on mitochondria. TBK1 in turn phosphorylates OPTN's UBAN domain at S473, thereby expanding the binding capacity of OPTN to diverse Ub chains. In combination with phosphorylation of S177 and S513, this posttranslational modification promotes recruitment and retention of OPTN/TBK1 on ubiquitinated, damaged mitochondria. Moreover, phosphorylation of OPTN on S473 enables binding to pS65 Ub chains and is also implicated in PINK1-driven and Parkin-independent mitophagy. Thus, TBK1-mediated phosphorylation of autophagy receptors creates a signal amplification loop operating in selective autophagy of damaged mitochondria.

mitophagy | TBK1 | OPTN | ubiquitin | phosphorylation

As a cell survival pathway, autophagy selectively frees the cytosolic compartment from bulky protein aggregates, invading bacteria or damaged organelles such as mitochondria and peroxisomes (1, 2). In this context, the posttranslational modifier ubiquitin (Ub) has been widely recognized as a selective signal driving autophagy of such cellular components and cargoes (3, 4). Recently, ubiquitin itself has been discovered to be phosphorylated to promote autophagic clearance of damaged mitochondria (mitophagy; reviewed in refs. 5 and 6). Ser/Thr kinase PINK1 phosphorylates S65 of Ub, which is critical for two steps of this process: allosteric activation of the E3 Ub ligase Parkin and recruitment of the autophagic machinery, including autophagy receptors (7–14).

Autophagy receptors function as decoders for the various ubiquitin signals on cargoes, linking cargoes to autophagosomal membranes (4); however, the basis of their individual recruitment to cargo as well as their distinct and cooperative functions in cargo sequestration are still poorly understood. The autophagy receptors optineurin (OPTN) and p62 are first activated by protein kinases to effectively target autophagic membranes or their polyUb cargo (15–17). TANK-binding kinase 1 (TBK1) phosphorylates OPTN on S177, thereby enhancing LC3-binding affinity and autophagic clearance of cytosolic *Salmonella* (15). Activity and specificity of TBK1 are defined by adaptor proteins; these recruit TBK1 to microdomains on ubiquitinated *Salmonella* or mitochondria, thereby facilitating its local clustering and activation (18), where it in turn can phosphorylate autophagy receptors (15). It is relevant to stress that a number of mutations in both OPTN and TBK1 have been identified in patients suffering from amyotrophic lateral sclerosis (ALS) and frontotemporal lobar degeneration (FTLD), which points toward an important role of the OPTN–TBK1 complex in autophagy and neurodegeneration (19–22).

Here, we provide evidence that TBK1 integrates upstream Ub-dependent signaling events by phosphorylating the autophagy receptor OPTN in the Ub-binding domain (UBD) in ABIN proteins and NEMO (UBAN), thus controlling its binding to Ub chains and regulating autophagy of damaged mitochondria. We also show that the ALS-associated mutant TBK1 E696K that is unable to bind to OPTN also fails to translocate to damaged mitochondria, highlighting an important role for OPTN in the regulation of TBK1.

Results

TBK1 Directly Phosphorylates the UBAN Domain of OPTN. TBK1 has been reported to regulate the autophagy receptors OPTN and p62 during bacterial infection (15, 17) and, more recently, during mitophagy (13, 23). We next used stable isotope labeling with amino acids in cell culture (SILAC)-based quantitative MS analysis to systematically identify TBK1-depedent phosphorylation sites on multiple autophagy receptors. To this end, SILAC-labeled HEK293T cells expressing GFP-tagged OPTN, NDP52, p62, or

Significance

Selective autophagy of damaged mitochondria (mitophagy) requires protein kinases PINK1 and TBK1, ubiquitin ligase Parkin, and autophagy receptors such as OPTN, driving ubiquitin-labeled mitochondria into autophagosomes. Because all proteins have been genetically linked to either Parkinson's disease (PINK1 and Parkin) or amyotrophic lateral sclerosis and frontotemporal lobar degeneration (TBK1 and OPTN), it is of great interest to understand their physiological functions. By utilizing quantitative proteomics we show that TBK1 phosphorylates four receptors on several autophagy-relevant sites. Constitutive interaction of TBK1 with OPTN and the ability of OPTN to bind to ubiquitin chains are essential for TBK1 recruitment and activation on mitochondria. TBK1-mediated phosphorylation of OPTN creates a signal amplification loop through combining recruitment and retention of OPTN/TBK1 on ubiquitinated mitochondria.

Author contributions: B.R., D.A.S., L.H., A.S., C.W., P.W., S.M., R.J.Y., and I.D. designed research; B.R., D.A.S., L.H., A.S., C.W., P.B., G.Z., P.W., and S.A.W. performed research; B.R., D.A.S., L.H., A.S., C.W., P.B., G.Z., P.W., S.M., S.A.W., R.J.Y., and I.D. analyzed data; and B.R., D.A.S., L.H., A.S., S.A.W., R.J.Y., and I.D. wrote the paper.

The authors declare no conflict of interest.

This article is a PNAS Direct Submission.

[1]Present address: Institute of Biochemistry, ETH Zürich, 8093 Zürich, Switzerland.

[2]To whom correspondence should be addressed. Email: ivan.dikic@biochem2.de.

This article contains supporting information online at www.pnas.org/lookup/suppl/doi:10.1073/pnas.1523926113/-/DCSupplemental.

TAX1BP1 were cotransfected with TBK1 WT or kinase-deficient (KD) mutant (TBK1 K38A). Autophagy receptors were enriched using affinity purification under denaturing conditions followed by MS analysis (Fig. S1*A*). By determining the relative abundance of phosphopeptides from cells expressing WT or KD TBK1, we were able to identify phosphorylation sites that are dependent on the active kinase. Surprisingly, TBK1 directly or indirectly mediates phosphorylation of all four receptors on multiple, autophagy-relevant sites, including the UBAN domain of OPTN, UBA domain of p62, SKICH domains of NDP52, and TAX1BP1 and LIR domains of OPTN and p62 (Fig. 1*A*). OPTN showed two prominent clusters of TBK1-regulated phosphosites: multiple phosphoserines adjacent to the LIR, including S177 as described previously (15), as well as multiple phosphosites located within (T460, T462, S473) or adjacent (S513) to the UBAN domain (Fig. 1*A*). The relative abundance of pS473 and pS513 was significantly increased in cells expressing TBK1 WT compared with KD, with pS513 being ∼4–5× more abundantly phosphorylated than pS473 (Fig. 1 *B* and *C*). Sequence analysis revealed that pS473 is in direct proximity to a conserved motif of the coiled-coil UBAN dimer ($_{474}$DFxxER$_{479}$; Fig. S1*B*) that is essential for Ub binding (15, 24–26). p62 phosphorylation sites were distributed over all domains, and in line with previous reports S403 was identified as being regulated by TBK1 (Fig. 1*A*) (16, 17).

To determine if recombinant TBK1 directly phosphorylates the UBAN domain of OPTN, we performed in vitro kinase assays. MS analysis revealed that TBK1 can directly phosphorylate multiple sites near the UBAN of OPTN, including S473 and S513 (Fig. S1*C*) and also as a positive control, S403 in the UBA of p62 (Fig. S1*D*) (17).

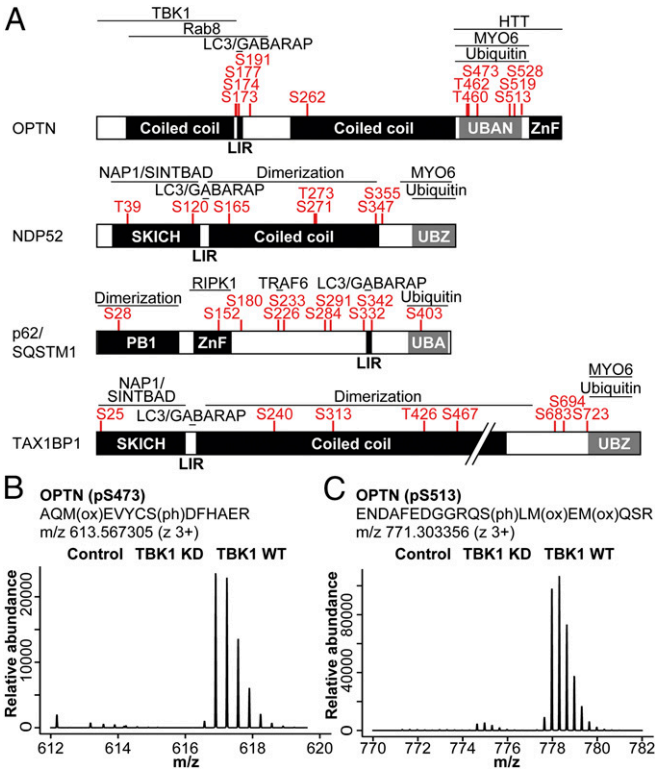

Fig. 1. TBK1 phosphorylates autophagy receptors on multiple, autophagy-relevant sites. (*A*) Domain structure and TBK1-dependent phosphorylation sites ($\log_2$TBK1 KD/TBK1 WT ≥ 1) of individual autophagy receptors. (*B* and *C*) Mass spectrometric parent ion scans of the peptides corresponding to pS473 and pS513 on OPTN with increased relative abundance of phosphorylated peptides in cells expressing WT TBK1.

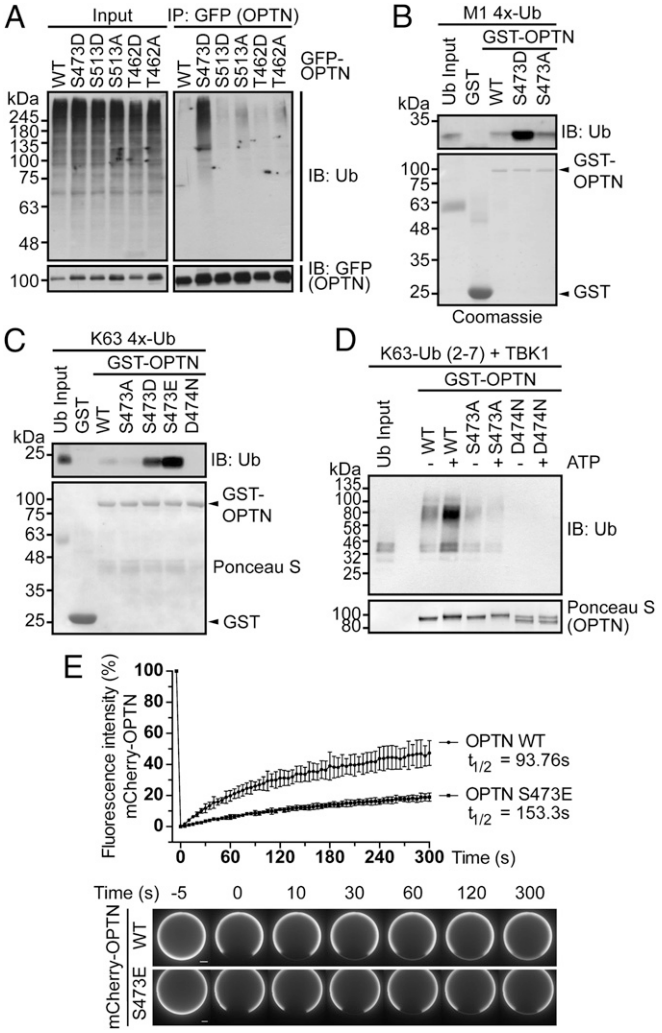

Fig. 2. Phosphorylated OPTN UBAN domain enhances binding to ubiquitin chains. (*A*) GFP immunoprecipitation of GFP–OPTN WT and indicated mutants from HEK293T cell lysates. (*B* and *C*) Indicated GST proteins were incubated with purified M1-linked (*B*) or K63-linked (*C*) tetra-Ub chains. (*D*) GST–OPTN WT and mutants were phosphorylated in vitro by TBK1 and subsequently incubated with purified Ub chains. Efficient phosphorylation of OPTN is indicated through an electrophoretic mobility shift. (*A*–*D*) Samples were subjected to immunoblot. Coomassie or Ponceau S staining show equal GST protein levels. (*E*) FRAP assay of recombinant mCherry–OPTN WT (●) or S473E (■) on the surface of diUb-conjugated beads (*Upper*). Images were taken before and after photobleaching at indicated time points (*Lower*). (Scale bar, 10 μm.)

Phosphorylation of OPTN's UBAN Domain Enhances Binding to Multiple Ubiquitin Chains. To test if any of the identified OPTN phosphorylation sites affect Ub binding in cells, we immunoprecipitated GFP–OPTN WT or the corresponding phosphomimetic mutants. Only OPTN S473, and none of the other identified sites, showed a detectable increase in affinity toward cellular polyUb proteins (Fig. 2*A* and Fig. S2*A*). When coexpressed with Myc-TBK1, GFP–OPTN WT showed increased capacity to coprecipitate polyUb proteins, but not in the presence of a TBK1 inhibitor (BX795; Fig. S2*B*). This effect indeed relied on phosphorylation of OPTN S473 because the mutant S473A was significantly reduced in its ability to bind polyUb proteins upon TBK1 coexpression (Fig. S2*C*, lanes 5 and 11) comparable to p62 when S403 is mutated to S403A (Fig. S2*D*, lanes 5 and 11) (16). Thus, phosphorylation of S473 is sufficient to increase the capacity of OPTN to bind to polyUb chains in cells.

To test Ub binding in vitro, we performed pull-down experiments with recombinant GST–OPTN and Ub chains. Until recently only M1- and K63-linked Ub chains were implicated in binding to OPTN (15, 23, 26). Phosphomimetic OPTN S473D bound significantly more potently to tetraUb chains than WT or S473A (Fig. 2 *B* and *C*), and also overcame the weak affinity toward K63-Ub, resulting in binding comparable to M1-linked Ub chains (Fig. S2*E*).

We then tested the binding of OPTN WT vs. S473E toward all available diUb chains. Whereas OPTN WT bound only weakly to short M1-diUb, we observed increased binding of OPTN S473E to nearly all Lys-linked chains (Fig. S2*F*). Ub chain length appears also important for binding to OPTN: whereas K63-diUb weakly bound to OPTN WT or S473E (Fig. S2*F*), longer K63-Ub chains potently bound to the phosphomimetic mutant OPTN S473D (Fig. S2*G*). Additionally, NEMO, if provided with a negative charge at the corresponding site in its UBAN (NEMO A310E), also more potently binds K63 polyUb chains (Fig. S2 *H* and *I*). To demonstrate that OPTN S473D/E functionally resembles pS473, we performed in vitro phosphorylation assays: OPTN WT but not S473A (Fig. 2*D*) showed an increase in Ub binding similar to OPTN S473D/E (Fig. 2 *B* and *C*). Similarly, pS473 OPTN purified from *Escherichia coli* using an orthogonal phosphoserine translation system (27) showed increased binding to Ub (Fig. S2*J*). Phosphorylation of OPTN at S177, S473, and S513 in cells was further confirmed, as visualized by an electrophoretic mobility shift of GFP–OPTN upon treatment with the phosphatase inhibitor calyculin A, which was lost if these sites were mutated to alanine (Fig. S2*K*).

To study the kinetics of pS473 OPTN to Ub binding, we performed time-lapse microscopy imaging in combination with fluorescence recovery after photobleaching (FRAP) using bacterially purified mCherry–OPTN WT or S473E and diUb-conjugated beads. Images were taken before and after photobleaching (Fig. 2*E*, *Lower*). The slower and reduced recovery of OPTN S473E after photobleaching compared with OPTN WT indicates that a negative charge at S473 leads to a more stable interaction with a lower molecular exchange rate. Indeed, the half-time of recovery for OPTN WT and S473E was 93.76 and 153.3 s, respectively, with a recovery rate of ∼45% and ∼20% (Fig. 2*E*, *Upper*). Thus, ∼80% of OPTN S473E remained immobile compared with ∼55% of OPTN WT, suggesting an increased residence time of OPTN S473E on diUb.

TBK1 Is Recruited to Mitochondria and Activated via OPTN Binding. TBK1 and OPTN act together downstream of the PINK1–Parkin pathway to facilitate the autophagic removal of damaged mitochondria (mitophagy) (13, 23). WT OPTN, but not an ALS-associated, Ub-binding deficient mutant (OPTN E478G) colocalized to and facilitated clearance of damaged mitochondria independent of p62 function (13, 28). In accordance, we demonstrate that endogenous TBK1 is activated (autophosphorylation of S172) upon treatment with antimycin A and oligomycin (AO) or carbonyl cyanide m-chlorophenylhydrazone (CCCP) in SH-SY5Y and HeLa cells after 45 min (Fig. 3 *A* and *B* and Fig. S3). Robust TBK1 activation relied on inducible expression of E3 Ub ligase Parkin in HeLa cells (Fig. 3*A*), indicating the existence of two distinct TBK1 activation pathways, Parkin dependent and Parkin independent. Increased activation of TBK1 upon Parkin overexpression is presumably connected to its interplay with OPTN, because stable recruitment of OPTN to mitochondria also depends on the presence of Parkin (28). Consistent with this hypothesis, overexpression of Parkin in OPTN KO HeLa cells did not lead to further activation of TBK1 (Fig. 3*C*). In contrast, knockdown of the protein kinase PINK1 completely abolished activation of TBK1, indicating an upstream role of this kinase in TBK1 activation, which is consistent with recent reports (Fig. 3*D*) (13, 23).

The N terminus of OPTN (amino acids 1–179) directly binds to the C-terminal adaptor-binding domain of TBK1 to form a stable complex in cells (29, 30). Mutagenesis of this domain indicates that OPTN binding may depend on the coiled-coil structure of TBK1

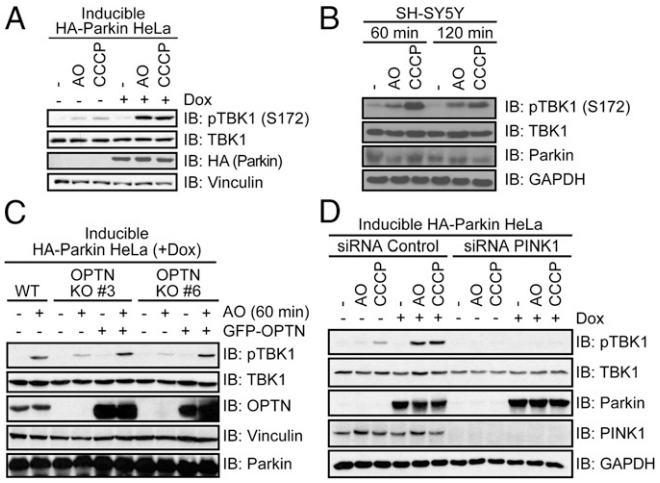

Fig. 3. TBK1 activation through mitophagy induction. (*A*, *C*, and *D*) Doxycycline (Dox)-inducible HA-Parkin HeLa cells were preincubated with Dox for 48 h before AO/CCCP treatment for (*A* and *D*) 80 min or (*C*) 60 min. (*B*) SH-SY5Y cells were treated with AO or CCCP for the indicated time. (*C*) WT or OPTN KO HeLa cells (nos. 3 and 6) stably expressing HA-Parkin were reconstituted with empty vector or GFP–OPTN for 30 h. (*D*) Cells were transfected with PINK1 or control siRNA for 48 h before treatment and lysis. (*A*–*D*) Cell lysates were subjected to immunoblot analysis with indicated antibodies. Active TBK1 was detected with a phosphospecific antibody (pTBK1 = pS172).

because several point mutations, including ALS-related missense mutation E696K, disrupt OPTN binding (Fig. S4 *A*–*C*). In addition to OPTN, TBK1 is able to bind Tank, Nap1, and Sintbad in a mutually exclusive manner (29, 30). Notably, OPTN is the only adaptor protein directly linking TBK1 to autophagy pathways. Whereas deletion of the complete adaptor-binding domain (Δ690–713) disrupts the interaction with all four adaptors, TBK1 E696K only inhibited binding to OPTN (Fig. S4 *D* and *E*).

To further analyze the importance of OPTN binding to TBK1 in mitophagy, we performed immunofluorescence experiments with TBK1 WT and E696K mutant (Fig. 4). Stable translocation of TBK1 to damaged, Parkin-positive mitochondria in HeLa cells was in most instances dependent on OPTN: whereas upon CCCP treatment, TBK1 WT was seen to border Parkin-positive mitochondria in over 90% of cells, this was true for less than 10% in case of TBK1 E696K (Fig. 4 and Fig. S4*F*). These findings point to a possible pathogenic role of defective mitophagy in ALS pathogenesis.

Phosphorylation of Ub on S65 Affects OPTN Binding. The protein kinase PINK1 phosphorylates S65 on Ub, which is critical for Parkin activation, and for recruitment of autophagy receptors OPTN and NDP52 to ubiquitinated mitochondria following their depolarization (7–14, 23). To investigate the binding behavior of OPTN to these phosphoUb species, we first expressed WT and phosphomimicking S65 Ub (S65E and S65D) together with OPTN in cells. Expression of phosphomimetic Ub led to an increase in coprecipitation with GFP–OPTN compared with WT or S65A mutant Ub (Fig. S5*A*) (13). However, the situation in vitro was different because phosphorylation of K63-linked Ub chains by PINK1 (stoichiometry of S65 phosphorylation of 0.5) reduced binding to GST–OPTN (Fig. S5*B*), which is consistent with previous findings when direct interactions were tested (31). Notably, phosphomimetic OPTN S473E and TBK1-phosphorylated OPTN could rescue the interaction and enabled moderate binding to pS65 Ub (Fig. S5 *B* and *C*). Although the reasons for the observed discrepancy in binding of OPTN to phosphorylated Ub are yet to be discovered, our findings indicate that phosphorylation of OPTN alone or in complex with other proteins may act as a mechanism to overcome the precluding effects of UBD binding to phosphorylated Ub in vivo.

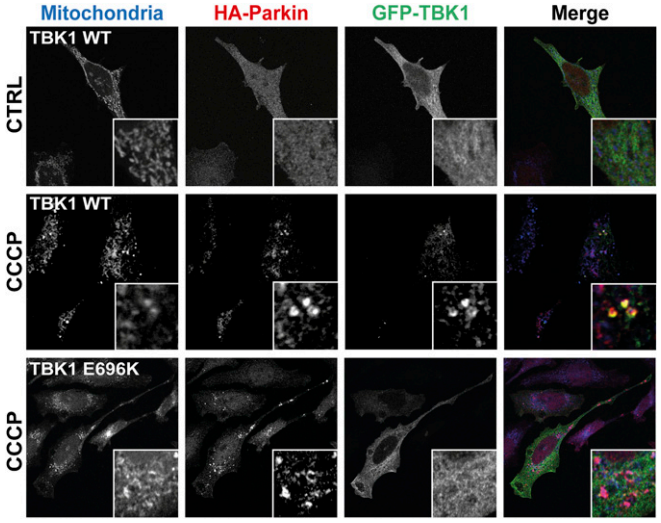

Fig. 4. OPTN–TBK1 complex formation is blocked by ALS-associated human mutations. Immunofluorescence of HeLa cells stably expressing HA-Parkin. Cells were transfected with GFP–TBK1 WT or E696K for 48 h and treated with CCCP for 105 min. Individual and merged images show mitochondria (blue), Parkin (red), and TBK1 (green).

Functional Characterization of OPTN Phosphorylation in Mitophagy. To test the functional consequence of TBK1-mediated phosphorylation of OPTN in mitophagy, pentaKO cells (HeLa cells engineered by CRISPR lacking NDP52, OPTN, TAX1BP1, NBR1, and p62) (13) were rescued with GFP–OPTN WT or mutants S473A, S513A, S473/S513A or phosphomimetics S473D, S513D, S473/S513D (Fig. S6 *A* and *B*). Following 0.5-h AO treatment, GFP–OPTN S473D translocated moderately better than WT, S513D translocated as well as WT, and the remaining mutants, GFP–OPTN S473A, S513A, S473/513A, and S473/513D translocated to mitochondria significantly slower than WT (Fig. 5*A* and Fig. S6*C*). After prolonged mitochondrial depolarization (3 h AO), WT and all mutants translocated to mitochondria, suggesting that UBAN phosphorylation may play important roles in early stages of mitophagy or in settings were ubiquitin is limited (Fig. 5*A* and Fig. S6*D*). TBK1 was activated to the same degree in these cells following AO treatment (Fig. S6*E*). We examined mitophagy using FACS analysis of mitochondrially targeted mKeima (mt-mKeima) (13, 32). The excitation spectrum of mKeima shifts when it is exposed to low pH, allowing measurement of the recruitment of mitochondria into lysosomes as a measure of mitophagy. Consistent with the lack of translocation defects at a later time point (Fig. 5*A* and Fig. S6*D*), all OPTN mutants could induce mitophagy to the same degree as OPTN WT (Fig. S7*A*).

A third and highly abundant TBK1-dependent phosphorylation site on OPTN, pS177, was recently shown to be also important for mitophagy (13). OPTN S177A localized poorly to mitochondria and only weakly restored mitophagy in pentaKO cells (13), indicating that pS177 may stabilize OPTN on ubiquitinated mitochondria. In pentaKO cells, GFP–OPTN S177/473/513D translocated significantly faster to mitochondria following 0.5-h AO treatment compared with WT, whereas translocation of GFP–OPTN S177/473/513A was significantly reduced (Fig. 5*B* and Fig. S7 *B–D*). After 3-h AO treatment, GFP–OPTN WT and S177/473/513D translocated to mitochondria in nearly every cell, but GFP–OPTN S177/473/513A translocation was decreased (Fig. 5*B* and Fig. S7 *C–E*). Mitophagy in HA–Parkin-expressing pentaKO cells was also significantly enhanced by expression of Flag/HA–OPTN S177/473/513D (Fig. 5 *C* and *D* and Fig. S8 *A–C*). Taken together, these data support a stabilizing role for TBK1 phosphorylation at S177 and a recruitment function for phosphorylation at S473 and S513.

To test if phosphomimetic OPTN is interacting with phosphorylated ubiquitin on mitochondria and not just unmodified ubiquitin added via Parkin activity, we studied OPTN translocation in cells

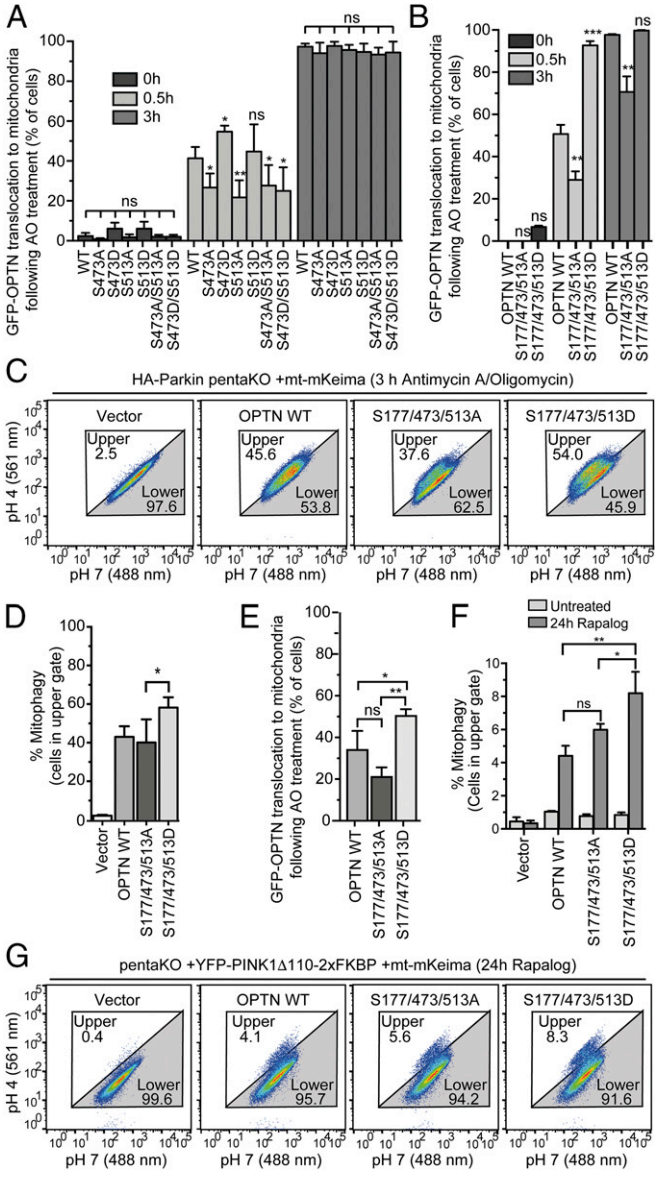

Fig. 5. OPTN translocation to mitochondria and mitophagy are enhanced by OPTN phosphomimetic mutations. (*A* and *B*) mCherry–Parkin pentaKO cells expressing GFP–OPTN WT or mutants were treated with AO for 0.5 or 3 h and immunostained for TOM20. Quantification of cells with GFP–OPTN colocalized with TOM20. For representative images, see Figs. S6 *C* and *D* and S7 *B* and *E*. (*C* and *D*) HA-Parkin pentaKO cells expressing mt-mKeima and vector, Flag/HA–OPTN WT or mutants, as indicated, were treated with AO for 3 h and analyzed by FACS for lysosomal-positive mt-mKeima. (*D*) Graph depicting the average percent of cells in the upper gate from FACS analysis in *C* ($n = 3$). (*E*) PentaKO cells expressing GFP–OPTN WT or mutants were treated with AO for 24 h. For representative images, see Fig. S8 *E* and *F*. (*F*) Graph depicting the average percent of cells in the upper gate from FACS analysis of pentaKO cells expressing PINK1Δ110-YFP-2xFKBP, mt-mKeima and vector, Flag/HA–OPTN WT, or mutants, following treatment with rapalog for 24 h ($n = 3$). (*G*) Representative FACS data from rapalog-treated conditions from *F* are shown. For *A*, *B*, and *E*, 100 cells per condition were counted for $n = 3$ experiments. For *A*, *B*, *D*, *E*, and *F*, data are presented as mean ± SD, $*P < 0.05$, $**P < 0.01$, $***P < 0.005$; ns, not significant. For the untreated conditions from *C* and *G*, see Fig. S8 *C* and *G*, respectively.

lacking Parkin expression. A previous study has shown that HeLa cells produce a truncated Parkin transcript lacking the 5′-end (exons 1–6) (33). We investigated this issue in more detail by identifying 5′ cDNA ends of the Parkin gene in HeLa cells using RLM-RACE. Specific PCR products of expected sizes were produced from 293T cDNA but not two HeLa cDNA samples (Fig. S8*D*), demonstrating that HeLa cells are truly null for Parkin at the transcriptional level. Thus, GFP–OPTN WT translocated to mitochondria in 32% of pentaKO HeLa cells following 24-h AO (Fig. 5*E* and Fig. S8 *E* and *F*), in strong contrast to Parkin-expressing cells, where GFP–OPTN translocates in nearly 100% of cells after 3-h AO (Fig. 5*B* and Fig. S7*E*), consistent with the model that PINK1 can directly recruit OPTN to mitochondria and that Parkin amplifies this pathway via ubiquitination. GFP–OPTN S177/473/513D translocated significantly more than both WT and S177/473/513A (Fig. 5*E* and Fig. S8 *E* and *F*), suggesting that phosphoUb preferentially recruits phosphomimetic OPTN relative to OPTN WT or nonphosphorylatable OPTN.

To study the effect of phosphomimetic OPTN on PINK1-driven, Parkin-independent mitophagy, we used an inducible PINK1 dimerization system. Here, PINK1 lacking its N-terminal membrane-targeting domain is fused to YFP and two tandem FKBP domains (PINK1-Δ110-YFP-2XFKBP). By the addition of rapalog, PINK1 is targeted to mitochondria that are stably expressing FKBP12/rapamycin-binding (FRB) fused to Fis1 (FRB–Fis1) (34); this allows PINK1, in the absence of Parkin and mitochondrial membrane depolarization, to phosphorylate mitochondrial ubiquitin to recruit autophagy receptors (13). Following rapalog treatment for 24 h, Flag-HA–OPTN WT induced mitophagy in 4.1% of cells, 10-fold more than without OPTN (vector, 0.4% of cells) and fivefold more than untreated conditions (0.9% of cells), consistent with previous reports (Fig. 5 *F* and *G* and Fig. S8 *G–I*) (13). Flag-HA OPTN S177/473/513A could rescue similar to OPTN WT with 5.6% of cells undergoing mitophagy, likely because TBK1 is not activated by rapalog to mediate phosphorylation of OPTN (Fig. S8*I*). Rescue with Flag-HA–OPTN S177/473/513D significantly increased mitophagy, to 8.3%, nearly doubling the mitophagy induced by OPTN WT (Fig. 5 *F* and *G*). GFP–OPTN S473/S513A and S473/513D rescued mitophagy similar to OPTN WT (Fig. S8 *J–L*), which again points toward a role for S473 and S513 phosphorylation at early steps in the process and highlights an important stabilizing function for S177.

Discussion

In the present study we have systematically analyzed the activity of TBK1 toward four major autophagy receptors. We found that TBK1 directly phosphorylates several autophagy-relevant sites in all four receptors, highlighting that TBK1 functions as a key player in the control of diverse selective autophagy pathways (5).

In line with two recent reports (13, 23), we confirmed that TBK1 is activated upon depolarization of mitochondria, an effect that requires the upstream kinase PINK1 and is further facilitated by the expression of Parkin. In addition, activation and mitochondrial localization of TBK1 depends on its interaction with OPTN and the ability of OPTN to bind to Ub on mitochondria (23). In turn, OPTN's function during mitophagy depends on its phosphorylation by activated TBK1, as demonstrated by a reduction in mitochondrial localization and mitophagy upon expression of nonphosphorylatable OPTN mutants. Both of these steps, TBK1 activation as well as OPTN recruitment and phosphorylation, seem to have a functional consequence for clearance of damaged mitochondria and cytosolic bacteria via feed-backward and feed-forward mechanisms (5).

Unphosphorylated OPTN was shown to interact primarily with M1-linked, and weaker with K63-linked, Ub chains (15, 26). In contrast TBK1-mediated phosphorylation of OPTN S473 or phosphomimetic S473D/E mutants resulted in increased binding and promiscuous interactions with multiple Lys-linked chain types (Fig. 2). Such a change in specificity can contribute to multivalent interaction and avidity-based increase in the residence time at the surface of ubiquitinated cargoes (Fig. 2*E*), indicative of an amplification loop rather than an on/off mechanism; this is also implicated in distinct stages of mitophagy, e.g., phosphorylation of OPTN appears to be critical in early steps of mitophagy, whereas in later steps OPTN phosphorylation is dispensable (Fig. 5). Moreover, only a subpopulation of OPTN can be modified on a specific site by locally enriched TBK1. Consistent with previous findings (23), we also show that the abundance of phosphorylated OPTN S473 is low if compared with S177 and S513 (Fig. 1), suggesting that its local enrichment in specific microdomains on mitochondria (23, 28) can determine the functional significance in vivo. Taken together, we propose that TBK1-mediated phosphorylation of OPTN is locally restricted to mitochondria and results in diversification of the binding spectrum of its UBAN domain toward distinct Ub chains, which in turn regulates its resident time on mitochondria and its function as an autophagy receptor (5).

In response to mitochondrial depolarization, PINK1 and Parkin establish a positive feedback loop that results in the robust decoration of damaged mitochondria with Ub chains that contain pS65 Ub (7–14). All tested autophagy receptors have been shown to translocate to damaged mitochondria; however, only OPTN and NDP52 seem to be required for efficient mitophagy in HeLa cells. Notably, whereas PINK1-mediated phosphorylation of Ub S65 increases the recruitment of autophagy receptors to damaged mitochondria in cells (Fig. 5) (13, 23), in vitro binding assays have shown opposite effects (Fig. S5) (23, 31). This obvious discrepancy can have several reasons. It could be that in vitro phosphorylated Ub chains show a different pattern of phosphorylation that does not match the in vivo situation. In fact, up to 20% of mitochondrial Ub is phosphorylated on S65 upon mitochondrial damage (7) and it is likely that Ub chains exposed to autophagy receptors consist of a mixture of pS65 Ub and unphosphorylated Ub. In this respect, if the effects seen in vitro apply to the situation in vivo, UBDs would favor unmodified Ub instead of pS65 Ub, and thereby preventing a competition with Parkin for pS65 Ub binding. However, TBK1 activation can result in phosphorylation of the UBAN domain and enhanced binding of OPTN to available S65 phosphorylated and unphosphorylated Ub chains that when coupled to TBK1-mediated phosphorylation of the LIR domain of OPTN supports early steps in mitophagy by stabilizing autophagic membranes on ubiquitinated cargo.

Previous studies identified mutations of OPTN, TBK1, and p62/SQSTM1 in patients with ALS–FTLD, an aggressive neurodegeneration characterized by the loss of upper and lower motor neurons, leading to rapid muscle weakness, paralysis, and death (19–22, 35). However, the spectrum of in vivo targets of autophagy in motor neurons remains unclear. Among possible targets are mutated superoxide dismutase 1 (SOD1) (36), the RNA-processing TAR DNA-binding protein 43 (TDP-43), fused in sarcoma (FUS), and mitochondria (13, 23). In a SOD1 mutant ALS mouse model, morphological abnormalities of mitochondria appeared before the onset of neurodegenerative symptoms, indicating a role for mitochondria in disease initiation (37). In cultured cells, we and others have shown that ALS-associated mutations in either TBK1 (E696K, abolishes OPTN binding) or OPTN (E478G, abolishes Ub binding) blocked mitochondrial translocation and activation of TBK1 resulting in impaired mitophagy (13, 23, 28). More studies are needed to dissect the contribution of selective autophagy pathways in the pathogenesis of ALS and other neurodegenerative diseases like Parkinson's disease (PD) where mutations in PINK1 and Parkin are causative to the development of disease. It remains intriguing that mutations in the same selective mitophagy pathway (PINK1-Parkin-OPTN-TBK1) have been genetically segregated to ALS (mutations in OPTN and TBK1) and to PD (PINK1 and Parkin), yet they share common principles of signal transduction, whereby kinases PINK1 and TBK1 initiate two independent amplification loops amplifying mitophagy by phosphorylating Ub and Ub receptors, respectively.

Materials and Methods

SILAC-IP and Phosphopeptide Identification. Lysates of SILAC-labeled HEK293T cells expressing GFP-tagged receptors were combined and incubated with GFP-Trap beads (ChromoTek) for 1 h, followed by washes under denaturing conditions (8 M Urea, 1% SDS in 1× PBS). Proteins were subjected to gradient SDS/PAGE gels followed by tryptic In-Gel digest. Extracted peptides were desalted and finally analyzed on a Hybrid Quadrupole-Orbitrap mass spectrometer. For details, see *SI Materials and Methods*.

Protein Expression and Purification. GST-fusion proteins were generated as described (15) with modifications. pSer473 OPTN was purified as described (27) with modifications. TBK1 was obtained from Merck Millipore. For details, see *SI Materials and Methods*.

FRAP Assay. GST–diUb bound to Glutathione Sepharose beads was incubated with purified mCherry–OPTN for 1 h. Subsequently, beads and proteins were dispensed in a 96-well plate for imaging with a spinning disk microscope. Three FRAP curves were generated for each experiment ($n = 2$) and sample. For details, see *SI Materials and Methods*.

Cell Culture, Cell Line Generation, and Knockdown. Inducible HA-Parkin HeLa cells were generated as described (38). OPTN KO and PentaKO HeLa cells were generated using CRISPR/Cas9 as described in refs. 39 and 13, respectively. For siRNA treatments, cells were reverse transfected with siRNAs against PINK1 or control using Lipofectamine RNAiMAX before treatment with AO. For details, see *SI Materials and Methods*.

Immunoprecipitation, Pull-Down, and Immunoblotting. Immunoprecipitation, pull-down, and immunoblotting were carried out as described (15) with modifications. For details and a listing of all antibodies, see *SI Materials and Methods*.

Mitochondrial Translocation Assays. GFP–OPTN translocation to mitochondria in pentaKO cells was assayed by immunofluorescence as described (13). PentaKO cells were treated with AO for times indicated and immunostained for TOM20. For details, see *SI Materials and Methods*.

Mt-mKeima Mitophagy Assay. Parkin-dependent and -independent mt-mKeima assays were performed by using FACS analysis as described in refs. 13 and 34, respectively. For details, see *SI Materials and Methods*.

ACKNOWLEDGMENTS. We thank Simin Rahighi and Masato Akutsu for helpful discussions; Evgenij Fiskin for the generation of HA-Parkin cells; Wade J. Harper and Alban Ordureau for purified pS65 Ub chains; Patricia Boya for mitophagy assays in mouse embryonic fibroblasts (MEFs); Giulio Superti-Furga for complementary DNA constructs; Jochen H. Weishaupt and Stephen Taylor for cells; and Dragan Maric and the National Institute of Neurological Disorders and Stroke (NINDS) Flow Cytometry Core for FACS. This work was supported by Deutsche Forschungsgemeinschaft Grant DI 931/3-1 (to I.D.); the Cluster of Excellence "Macromolecular Complexes" of the Goethe University Frankfurt (EXC115; to I.D.); LOEWE Grant Ub-Net (to I.D.) and LOEWE Centrum for Gene and Cell Therapy Frankfurt (I.D. and B.R.); the NIH-NINDS intramural program (R.J.Y., D.A.S., and C.W.); and an European Molecular Biology Organization (EMBO) long-term postdoctoral fellowship (to L.H.).

1. Ohsumi Y (2014) Historical landmarks of autophagy research. *Cell Res* 24(1):9–23.
2. Levine B, Mizushima N, Virgin HW (2011) Autophagy in immunity and inflammation. *Nature* 469(7330):323–335.
3. Kirkin V, McEwan DG, Novak I, Dikic I (2009) A role for ubiquitin in selective autophagy. *Mol Cell* 34(3):259–269.
4. Stolz A, Ernst A, Dikic I (2014) Cargo recognition and trafficking in selective autophagy. *Nat Cell Biol* 16(6):495–501.
5. Herhaus L, Dikic I (2015) Expanding the ubiquitin code through post-translational modification. *EMBO Rep* 16(9):1071–1083.
6. Pickrell AM, Youle RJ (2015) The roles of PINK1, parkin, and mitochondrial fidelity in Parkinson's disease. *Neuron* 85(2):257–273.
7. Ordureau A, et al. (2014) Quantitative proteomics reveal a feedforward mechanism for mitochondrial PARKIN translocation and ubiquitin chain synthesis. *Mol Cell* 56(3): 360–375.
8. Kane LA, et al. (2014) PINK1 phosphorylates ubiquitin to activate Parkin E3 ubiquitin ligase activity. *J Cell Biol* 205(2):143–153.
9. Kazlauskaite A, et al. (2014) Parkin is activated by PINK1-dependent phosphorylation of ubiquitin at Ser65. *Biochem J* 460(1):127–139.
10. Koyano F, et al. (2014) Ubiquitin is phosphorylated by PINK1 to activate parkin. *Nature* 510(7503):162–166.
11. Wauer T, et al. (2015) Ubiquitin Ser65 phosphorylation affects ubiquitin structure, chain assembly and hydrolysis. *EMBO J* 34(3):307–325.
12. Swaney DL, Rodríguez-Mias RA, Villén J (2015) Phosphorylation of ubiquitin at Ser65 affects its polymerization, targets, and proteome-wide turnover. *EMBO Rep* 16(9): 1131–1144.
13. Lazarou M, et al. (2015) The ubiquitin kinase PINK1 recruits autophagy receptors to induce mitophagy. *Nature* 524(7565):309–314.
14. Kazlauskaite A, et al. (2015) Binding to serine 65-phosphorylated ubiquitin primes Parkin for optimal PINK1-dependent phosphorylation and activation. *EMBO Rep* 16(8):939–954.
15. Wild P, et al. (2011) Phosphorylation of the autophagy receptor optineurin restricts Salmonella growth. *Science* 333(6039):228–233.
16. Matsumoto G, Wada K, Okuno M, Kurosawa M, Nukina N (2011) Serine 403 phosphorylation of p62/SQSTM1 regulates selective autophagic clearance of ubiquitinated proteins. *Mol Cell* 44(2):279–289.
17. Pilli M, et al. (2012) TBK-1 promotes autophagy-mediated antimicrobial defense by controlling autophagosome maturation. *Immunity* 37(2):223–234.
18. Helgason E, Phung QT, Dueber EC (2013) Recent insights into the complexity of Tank-binding kinase 1 signaling networks: The emerging role of cellular localization in the activation and substrate specificity of TBK1. *FEBS Lett* 587(8):1230–1237.
19. Freischmidt A, et al. (2015) Haploinsufficiency of TBK1 causes familial ALS and frontotemporal dementia. *Nat Neurosci* 18(5):631–636.
20. Maruyama H, et al. (2010) Mutations of optineurin in amyotrophic lateral sclerosis. *Nature* 465(7295):223–226.
21. Pottier C, et al. (2015) Whole-genome sequencing reveals important role for TBK1 and OPTN mutations in frontotemporal lobar degeneration without motor neuron disease. *Acta Neuropathol* 130(1):77–92.
22. Cirulli ET, et al.; FALS Sequencing Consortium (2015) Exome sequencing in amyotrophic lateral sclerosis identifies risk genes and pathways. *Science* 347(6229): 1436–1441.
23. Heo JM, Ordureau A, Paulo JA, Rinehart J, Harper JW (2015) The PINK1-PARKIN mitochondrial ubiquitylation pathway drives a program of OPTN/NDP52 recruitment and TBK1 activation to promote mitophagy. *Mol Cell* 60(1):7–20.
24. Wagner S, et al. (2008) Ubiquitin binding mediates the NF-kappaB inhibitory potential of ABIN proteins. *Oncogene* 27(26):3739–3745.
25. Rahighi S, et al. (2009) Specific recognition of linear ubiquitin chains by NEMO is important for NF-kappaB activation. *Cell* 136(6):1098–1109.
26. Gleason CE, Ordureau A, Gourlay R, Arthur JS, Cohen P (2011) Polyubiquitin binding to optineurin is required for optimal activation of TANK-binding kinase 1 and production of interferon β. *J Biol Chem* 286(41):35663–35674.
27. Heinemann IU, et al. (2012) Enhanced phosphoserine insertion during *Escherichia coli* protein synthesis via partial UAG codon reassignment and release factor 1 deletion. *FEBS Lett* 586(20):3716–3722.
28. Wong YC, Holzbaur EL (2014) Optineurin is an autophagy receptor for damaged mitochondria in parkin-mediated mitophagy that is disrupted by an ALS-linked mutation. *Proc Natl Acad Sci USA* 111(42):E4439–E4448.
29. Morton S, Hesson L, Peggie M, Cohen P (2008) Enhanced binding of TBK1 by an optineurin mutant that causes a familial form of primary open angle glaucoma. *FEBS Lett* 582(6):997–1002.
30. Goncalves A, et al. (2011) Functional dissection of the TBK1 molecular network. *PLoS One* 6(9):e23971.
31. Ordureau A, et al. (2015) Defining roles of PARKIN and ubiquitin phosphorylation by PINK1 in mitochondrial quality control using a ubiquitin replacement strategy. *Proc Natl Acad Sci USA* 112(21):6637–6642.
32. Bingol B, et al. (2014) The mitochondrial deubiquitinase USP30 opposes parkin-mediated mitophagy. *Nature* 510(7505):370–375.
33. Denison SR, et al. (2003) Alterations in the common fragile site gene Parkin in ovarian and other cancers. *Oncogene* 22(51):8370–8378.
34. Lazarou M, Jin SM, Kane LA, Youle RJ (2012) Role of PINK1 binding to the TOM complex and alternate intracellular membranes in recruitment and activation of the E3 ligase Parkin. *Dev Cell* 22(2):320–333.
35. Fecto F, et al. (2011) SQSTM1 mutations in familial and sporadic amyotrophic lateral sclerosis. *Arch Neurol* 68(11):1440–1446.
36. Korac J, et al. (2013) Ubiquitin-independent function of optineurin in autophagic clearance of protein aggregates. *J Cell Sci* 126(Pt 2):580–592.
37. Kong J, Xu Z (1998) Massive mitochondrial degeneration in motor neurons triggers the onset of amyotrophic lateral sclerosis in mice expressing a mutant SOD1. *J Neurosci* 18(9):3241–3250.
38. Tighe A, Staples O, Taylor S (2008) Mps1 kinase activity restrains anaphase during an unperturbed mitosis and targets Mad2 to kinetochores. *J Cell Biol* 181(6):893–901.
39. Ran FA, et al. (2013) Genome engineering using the CRISPR-Cas9 system. *Nat Protoc* 8(11):2281–2308.
40. Michalski A, et al. (2011) Mass spectrometry-based proteomics using Q Exactive, a high-performance benchtop quadrupole Orbitrap mass spectrometer. *Mol Cell Proteomics* 10(9):M111.011015.
41. Cox J, Mann M (2008) MaxQuant enables high peptide identification rates, individualized p.p.b.-range mass accuracies and proteome-wide protein quantification. *Nat Biotechnol* 26(12):1367–1372.
42. Cox J, et al. (2011) Andromeda: A peptide search engine integrated into the MaxQuant environment. *J Proteome Res* 10(4):1794–1805.
43. Zhu X, et al. (2014) An efficient genotyping method for genome-modified animals and human cells generated with CRISPR/Cas9 system. *Sci Rep* 4:6420.